

Experimental study of the instability of vortex rings.

A.Dazin, P.Dupont, M.Stanislas.
Ecole Centrale de Lille, L.M.L URA CNRS 1441
Laboratoire de Mécanique des Fluides
Cité scientifique BP 48
F 59651 Villeneuve d'Ascq CEDEX
Email : antoine.dazin@ec-lille.fr

ABSTRACT

The results of a series of experiments performed to study the development of instabilities in vortex rings are presented. The experiments were performed in water. The vortex rings are generated by pushing water throughout the cylindrical nozzle of a pipe, plunged in an aquarium. The Reynolds number of the vortices vary from 2650 to 6500. The experiments were made with the help of tomoscopic visualisation and Particle Image Velocimetry. Records are available in the symmetry plane of the vortex ring and in a plane normal to its axis. The results evidence two phases during the development of the instability: a linear and a non-linear phase. During the first phase, the tomoscopic images evidence patterns, which are typical of a periodic instability. The link between these patterns and the development of a three dimensional azimuthal wave is demonstrated with the help of a geometrical model (figure1). The PIV data are in agreement with the tomoscopic visualisations by showing also an azimuthal wave around the vortex rings. The number of waves inside the vortex is an agreement with theoretical models. The non-linear phase, which leads to the destruction of the vortex ring, is characterised by the development of secondary vortical structures, particularly in the median plane of the vortex (figure 2).

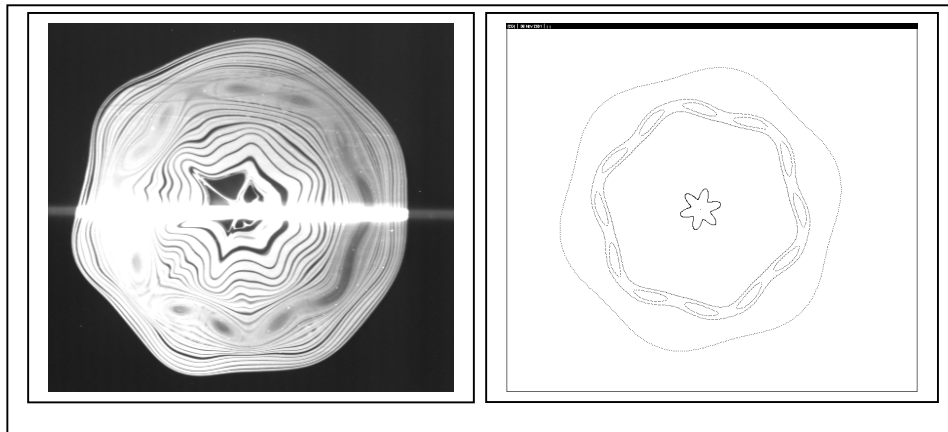


Figure 1 : Linear phase of the instability.

Comparison between visualisation and geometrical model in the median plane of the vortex

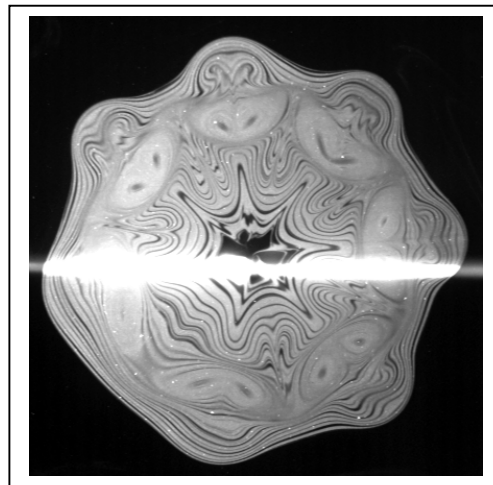


Figure 2 : Non linear phase of the instability in the median plane of the vortex

Nomenclature

a = vortex core radius

R = vortex radius

n = number of unstable waves

k = wavenumber

Γ = circulation of the ring

U_0 = propagation speed of the ring

U_p = piston average velocity

L_p = piston stroke

D_p = tube inner diameter

$Re_p = \frac{U_p D_p}{\nu}$ = Reynolds based on the piston velocity and the tube diameter

$Re_0 = \frac{2RU_0}{\nu}$ = Reynolds based on the propagation velocity and the radius of the vortex

1-Introduction

Generating a vortex ring is fairly easy. It can be done just by pushing fluid throughout a circular orifice. Thus, the vortex ring has become naturally a classical illustration of many subjects in fluid mechanics: formation of vortices (Didden (1979); Glezer (1988)); vortex interaction (Chu & Falco (1988), Orlandi & Verzicco (1993)) and vortex stability (Saffman (1978), Saffman (1981)). Maxworthy (1972) notices that, whereas at low Reynolds number (i.e. $Re_0 < 600$) stable vortex rings are formed, at higher Reynolds number an azimuthal wave develops and grows until the destruction of the vortex. Maxworthy (1977) confirmed that stagnant, non-rotating wave grows at 45° relative to the direction of propagation of the ring. Widnall et al (1973) and Sullivan & Widnall (1973) report an experimental study combining LDV and visualisation. They observe unstable vortices with different number of waves n . They compare n with the vortices characteristics (circulation Γ , speed of propagation U_0). Meng (1995) measured the velocity field of an unstable vortex ring with Holographic Particle Image Velocimetry. The correct theoretical explanation of the phenomenon was given soon after the first experimental observations : while Maxworthy (1972) was suggesting that the instability could be due to the vorticity produced at the edge of the tube, just after the formation of the vortex ring, Widnall et al (1973) did show that the vortex is unstable because of its structure. Their study was inspired by contributions made on the instability of a pair of vortex filament (Crow (1970)) or of the instability of a vortex filament in a strain field (Tsai & Widnall (1976)). Those three cases are somehow similar: in both cases a small perturbation may be amplified because of the existence of a straining field in the neighbourhood of the vortex core. This straining field is due to the presence of the second vortex in the case of a pair of vortex filament or to the curvature of the vortex in the case of the ring. These studies were based on an asymptotic analysis of a vortex of small core ($a \ll R$) and with a wavelength long compared to the vortex core ($ka \ll 1$). They show the existence of a three-dimensional azimuthal wave around the vortex and predict the number of waves n as a function of Γ and U_0 . There is an overall agreement between this theory and the existing experimental observations, but a noticeable difference remains on the prediction of the number of waves in the unstable mode. This is mainly due to the long waves hypothesis which does not fit the intermediate instability wavenumber ($ka \sim 1$) of most experiments. Widnall et al (1974) understand it well and give a simplified explanation of the mechanism of the instability. They suggest for the first time theoretically that the direction of the instability should be at 45° with the direction of propagation of the vortex. Widnall & Tsai (1977) give the rigorous theory, which predicts the number of waves and the growth rates for thin-core vortex rings with constant vorticity or with a continuous distribution of vorticity. Shariff et al (1994), in a numerical study, confirm those results and give a viscous correction to the growth rate.

As can be seen, all the approaches to the instability of the vortex ring indicate the existence of a three dimensional phenomenon. It was thus of interest to take this fact into account in the design of an experimental study. This is the aim of the work presented in this paper : a visualisation by video tomography and a PIV experiment have been performed in two simultaneous planes cutting vortex rings with a large viscous core. These experiments were performed with two main goals: to compare the linear phase of the instability with theory and to try to characterise the non-linear phase of the instability.

The experimental set-up is presented in section 2. Section 3 presents the experimental results in the linear phase. Section 4 presents a discussion on these results: a geometrical model is proposed to understand the

patterns observed during the experiments and a comparison is made between the experimental results and the theoretical predictions. Section 5 presents the tomoscopic images of the non-linear phase of the instability.

2-Experimental set up

The experiments are performed in water. The vortex rings are generated by pushing fluid throughout the cylindrical nozzle of a pipe, which is plunged into an aquarium (2.4m*0.6m*0.6m). The inner diameter of the pipe is $D_p = 35$ mm. The pipe is connected to a pressurised tank. Between the pipe and the tank, an electromagnetic valve opens the circuit for an adjustable duration. A polystyrene piston has also been fitted into the pipe in order to isolate the flow in the aquarium from the perturbations of the generating system. The stroke of this piston is adjustable. By setting the tank pressure and the opening time of the valve, it is possible to control the velocity of the piston (figure 3).

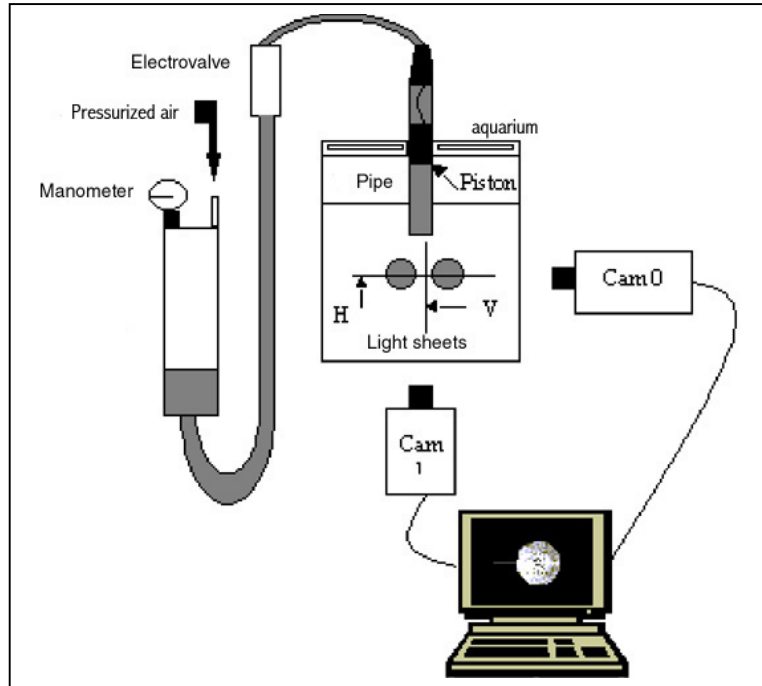


Figure 3: Experimental set-up

The average piston velocity can be varied from $U_p = 75$ mm/s to $U_p = 175$ mm/s and the stroke to nozzle-diameter ratio from $L_p/D_p = 1.25$ to $L_p/D_p = 2.5$. So, the Reynolds number $Re_p = (U_p * D_p) / \nu$ is varying from 2650 to 6100. The observations are made with the help of tomoscopic visualisation and Particle Image Velocimetry. Table 1 and table 2 give the injection characteristics of the vortices produced for respectively the visualisation experiments and the PIV experiments.

	U_p (mm/s)	L_p / D_p	Re_p
A	110	1.25	3800
B	145	1.25	5125
C	140	1.95	4900
D	75	2.4	2650
E	110	2.5	3800
F	145	2.5	5070
G	175	2.5	6100

Table 1: Tomoscopic experiments: injection characteristics

	U_p (mm/s)	L_p / D_p	Re_p
A'	100	1.25	3500
C'	132	1.9	4600

Table 2: PIV experiment: injection characteristics

Records were obtained in the symmetry plane of the vortex ring (V) and in a plane normal to its axis (H). The laser sheets were generated with a 5W Argon Ion laser (Spectra-Physics Series 2000 Ion Laser System) for tomoscopic visualisations and a 2*300 mJ BMI pulsed YAG laser for PIV. The video recordings were made with two identical CCD cameras (Pulnix TM-9701, 768*484 pixels, 30 Hz framing rate). One was placed on one side of the aquarium and the other one was under the aquarium. The video signals were digitized by means of an ICPCI board plugged in a PC computer (figure 1).

The visualisation results are sets of simultaneous images in the two planes, taken at a rate of 30 Hz, showing the different steps of the instability.

In PIV, cross-correlation was used with a correlation window size of 32 * 32 pixels and an overlapping of 50%. Correlation peaks were fitted with a three points gaussian model. The results consist of fields of 48*26 velocity vectors with a temporal resolution of 15 fields per second. The field of view is 195*150 mm² in the symmetry plane (V) and 110*85 mm² in the plane normal to the axis (H).

3-Results for the linear phase of instability

3.1-Tomoscopic observations

In this subsection, the tomoscopic observations for the linear phase are presented. Their interpretation in term of a three dimensional instability is given in next subsection.

The time origin is at the opening of the electrovalve. In each figure are given the time t of the record and the non-dimensional position $z_c = z/R$ of the H plane of observation with respect to the median plane of the vortex (Figure 4).

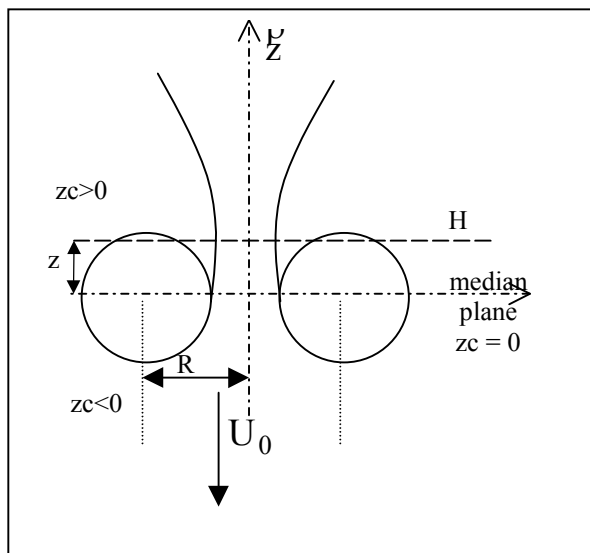


Figure 4: vortex characteristics

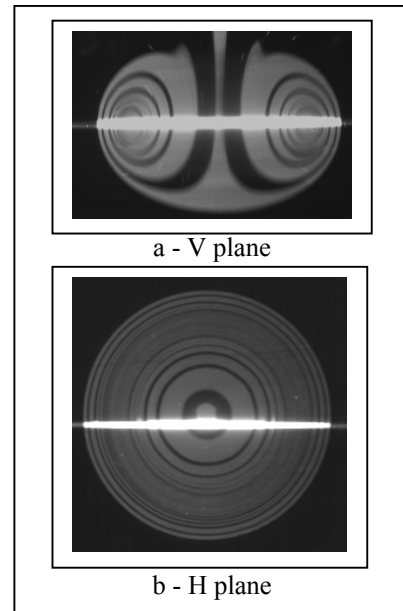


Figure 5: stable vortex $t = 1.83$ s $z_c = 0$

Consequently, z_c is positive in the downstream part of the vortex and negative in the upstream part. The results are presented here for only one value of the characteristic parameters ($Re_p = 3800$, $L_p / D_p = 2.5$) but the observations for the other values are similar.

When the vortex is stable, a series of concentric circles (dye / no dye alternance) can be observed in the H plane (figure 5b). They correspond to the spirals, classically observed in the V plane (figure 5a). When the instability develops, it is mainly observable in the H plane. Two phenomena occur during the linear phase: a deformation of the outer and inner lines of the vortex and the appearance of several characteristic patterns (named here type I to type VI) which are typical of the sinusoidal instability. The number of those patterns gives the number of waves n of the unstable perturbation. These shapes of instability patterns depend on the location of the H plane inside the vortex and on the time t of observation which is related to the evolution stage of the instability.

In the upstream part of the vortex ($z_c < 0$), the instability starts with a deformation of the concentric circles. The outer ones look like polygons and the inner ones take the shape of stars with branches stretching toward the outer border of the vortex (figure 6a). Between the branches, the type I patterns, looking like smooth triangles, do appear (figure 6b).

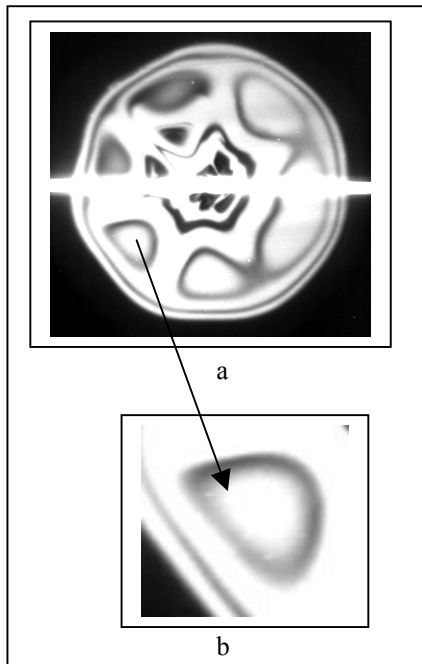


Figure 6: Type I $t=4.1s$ $z_c=-0.56$

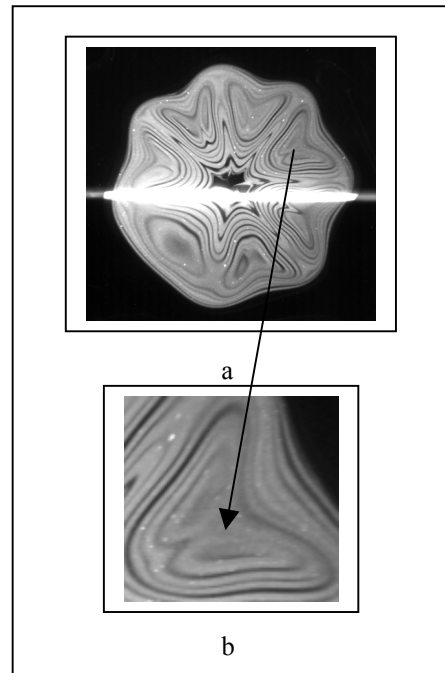
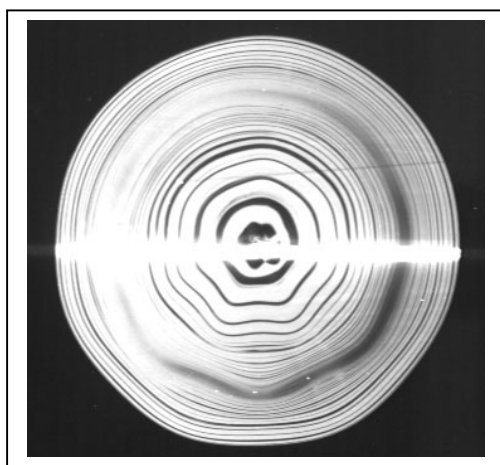


Figure 7: type II $t=5.7s$ $z_c = -0.31$

Later and nearer to the median plane, the type I patterns turn into type II which have something like a heart shape (figure 7 a, b). In the median plane, the beginning of the instability is also characterised by the deformation of the concentric circles into polygons, but all through the vortex. The deformation is far more visible for the inner lines than for outer ones. (figure 8)



**Figure 8: Instability in the median plane
 $t = 3.67s$ $z_c = 0$**

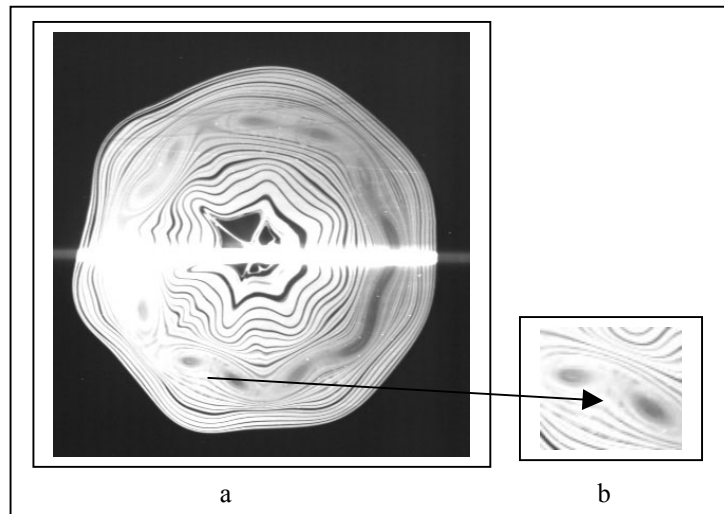


Figure 9: type III $t = 4.33s$ $z_c = 0$

Later in time, in this median plane, the dye lines surrounding the cores of the vortex link to form little patterns (type III) which number is twice the number of waves of the unstable mode (figure 9 a et b). At the same time, the inner circles take the shape of a star (figure 9a), like in figure 5 and 6.

In the downstream part of the vortex ($z_c > 0$), the instability starts also with a deformation of the outer lines similar to the one in the lower part. The inner lines shape rapidly into petals (figure 10a). In the middle part of the vortex, dye lines join to form nearly circular patterns (type IV, figure 10b).

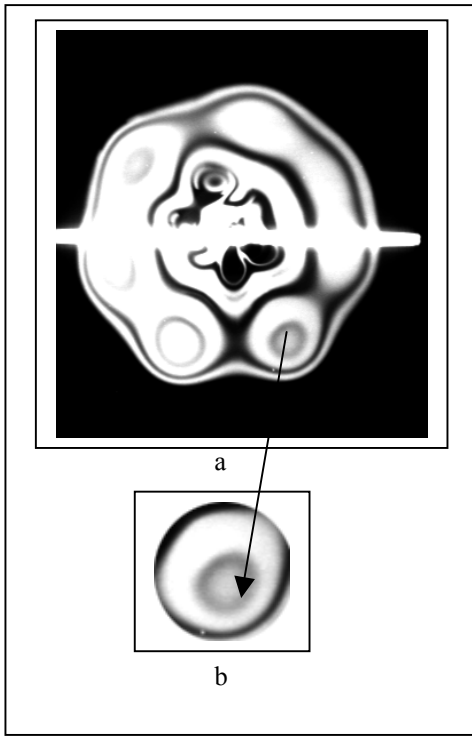


Figure 10: Type IV $t=3.97$ s $z_c=0.58$

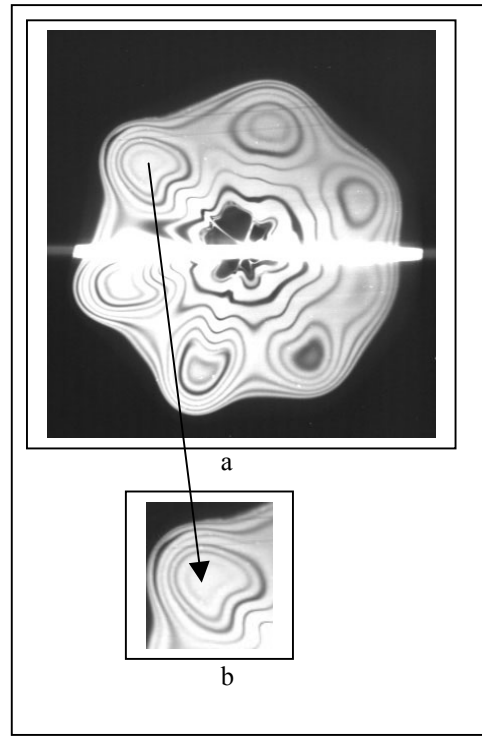


Figure 11: Type V $t = 4.53$ s $z_c = 0.41$

Later in time, the type IV patterns turn into Type V (figure 11b) which have again a heart shape but pointing outward instead of inward like in figure 7. The instability is detectable in the wake of the vortex too. There, it becomes rapidly organised into petals (type VI of figure 12 b).

In the (V) plane, along the whole linear stage, the instability is not really obvious. The comparison of the images of an unstable vortex (figure 12 a) with that of a stable vortex (figure 5a) shows just a slight dissymmetry between the two sides of the vortex and a bit of mixing of the dye lines inside the core

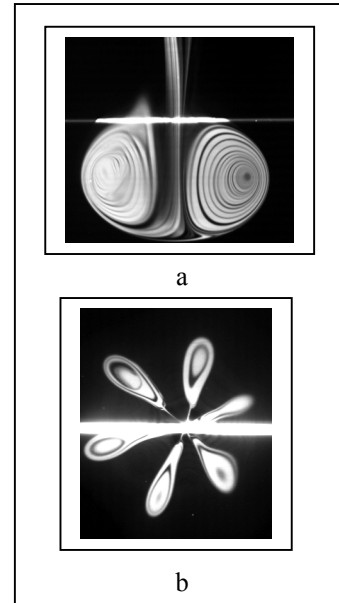


Figure 12: Type VI $t=4.77$ s $z_c = 0.82$

3.2 PIV results

As PIV is heavier to operate and analyse than simple visualisation, and as the tomoscopic visualisation did show that the main features observed were common to all cases but at different times, the PIV results were performed only for cases A' and C'. Preliminary results are presented here only for case A'. As a powerful Yag laser was used, no seeding was needed. The micron particles naturally present in tap water do provide a homogeneous seeding with a light power of about 200mJ/pulse and a light sheet cross section of 15 cm*2mm. For each case, the experiment was repeated 6 times and series of single exposed PIV images were recorded at a rate of 15 velocity fields/s. This, in the horizontal plane, allows to obtain about 25 maps inside the vortex.

Results are shown here only for the linear phase of the instability. Figure 13 gives two samples of radial velocity maps in the upstream and downstream parts of the vortex. During this linear phase, an azimuthal wave is clearly noticeable in these PIV radial velocity fields.

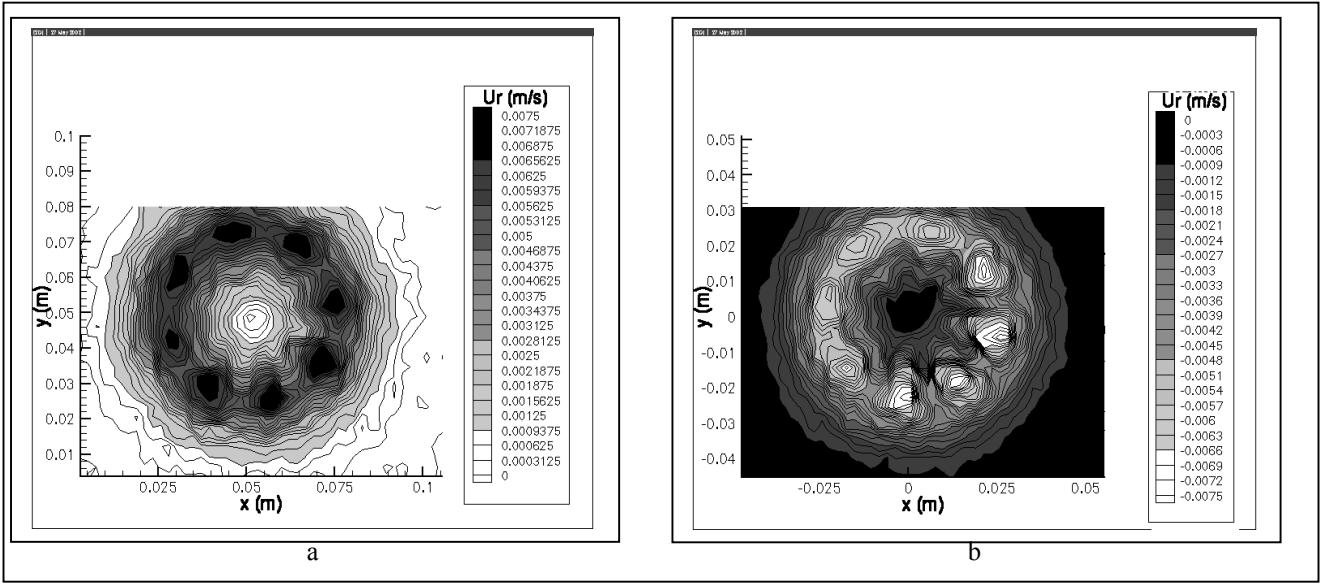


Figure 13: Radial velocity of an unstable vortex; (a) for $z_c = -0.31$ and (b) for $z_c = 0.47$

4-Discussion

4.1- Geometrical model

At this stage, the internal structure of the unstable vortex appears quite complex, although in the very early phase of the instability. And it is thus worth to try to link these observations with the prediction of the available theory. As these theories do all predict the development of a sinusoidal unstable mode, an attempt was made to model the result of such an instability in the tomographic visualisation. For that purpose, a simple geometrical model was developed in order to interpret the patterns observed in the tomographic images. This model consists in the sinusoidal deformation of a torus by an azimuthal three-dimensional wave.

The equation in cylindrical coordinates for a torus is (centre O (0,0,0), torus radius R, core size σ) :

$$z^2 + (R - r)^2 = \sigma^2 ; \text{ the locus of the core centres is a circle having the equations: } \begin{cases} r = R \\ z = 0 \end{cases}$$

A perturbation ε is then introduced. Its direction is along $(\hat{u}_r - \hat{u}_z)$ that is at 45° with the axis of the ring (OZ) as indicated by the theory.

Let n be the number of waves of the perturbation;

The equation for the core centres becomes: $\begin{cases} r = R_0 + \varepsilon \sin(n\theta) \\ z = -\varepsilon \sin(n\theta) \end{cases}$ and the equation of the distorted torus writes:

$$(z - \varepsilon \sin(n\theta))^2 + ((R_0 + \varepsilon \sin(n\theta)) - r)^2 = \sigma^2$$

It is then easy to cut this distorted torus by planes normal to OZ and located at different z_c . If this is the real instability developing in the vortex, the patterns observed should not be far from what is evidenced by the dye lines. The results are presented figure 14 for $n=6$ for different values of z_c .

The ring radius is one; and the results are presented for various values of σ and ε .

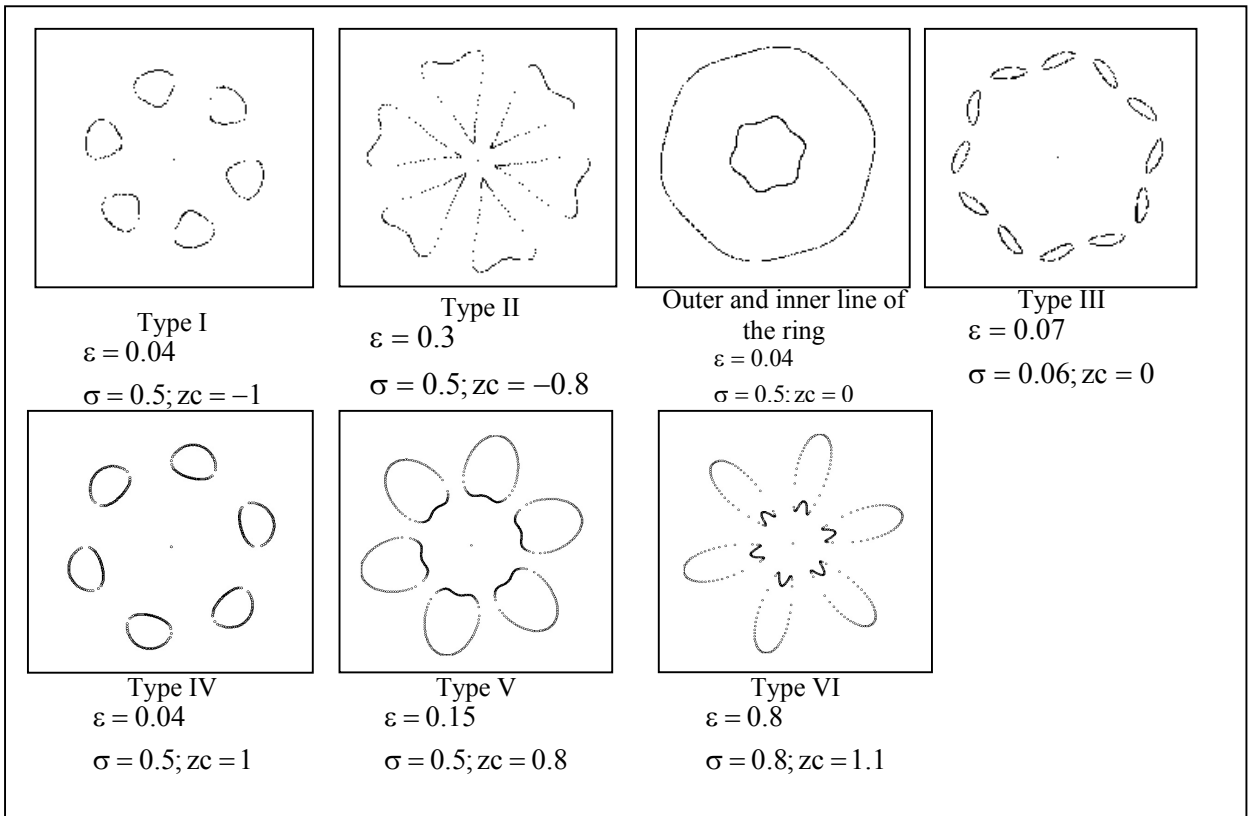


Figure 14: Various patterns obtained with the geometrical model

By combining several torus with different radius, it is possible to get shapes, which fits very well with the tomographic images. (figure 15)

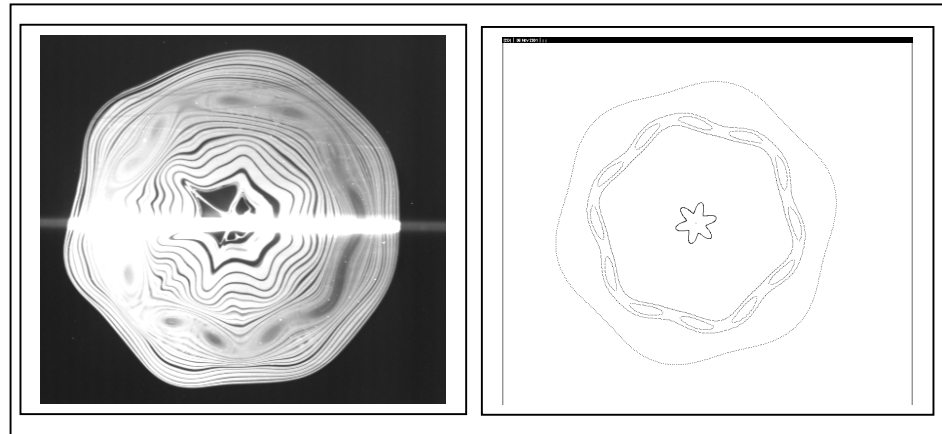


Figure 15: Comparison between an experimental image and a result obtained with the model

As can be observed, all the patterns observed by visualisation can be recovered by this simple model, demonstrating the existence of the three dimensional unstable mode predicted by theory.

4.2-Comparison of the number of waves with literature

The linear stability theory does not predict only the shape of the perturbation. Widnall & Tsai (1977) give a theoretical value of the number of waves n of the most unstable mode as a function of \tilde{V} a non-dimensional parameter depending on the velocity of the vortex, its radius and its circulation: $\tilde{V} = \frac{U_0}{\Gamma/4\pi R}$

Those results are obtained for thin vortices of constant vorticity or with a continuous variation of vorticity in the core (in this case, the distribution of vorticity in the core is $\omega(r_1) = (r_1^2 - a^2)^2$ with r_1 the distance from a core centre).

To compute the circulation of the vortex in the present experiment, PIV results in the V plane were used. By integrating the velocity along the axis of the vortex far enough from it on both sides, one has direct access to the circulation. The characteristics obtained in case A' are reported in table 3.

Γ (m ² /s)	U_0 (cm/s)	R (cm)	\tilde{V}	n
$6.1 \cdot 10^{-3}$	5.9	2.5	3	8

Table 3: Vortex characteristics

The results for this case are in good agreement with the theory (figure 16). This should be emphasised as the theory is established for thin core vortices whereas the core of the ring experimentally studied here is large.

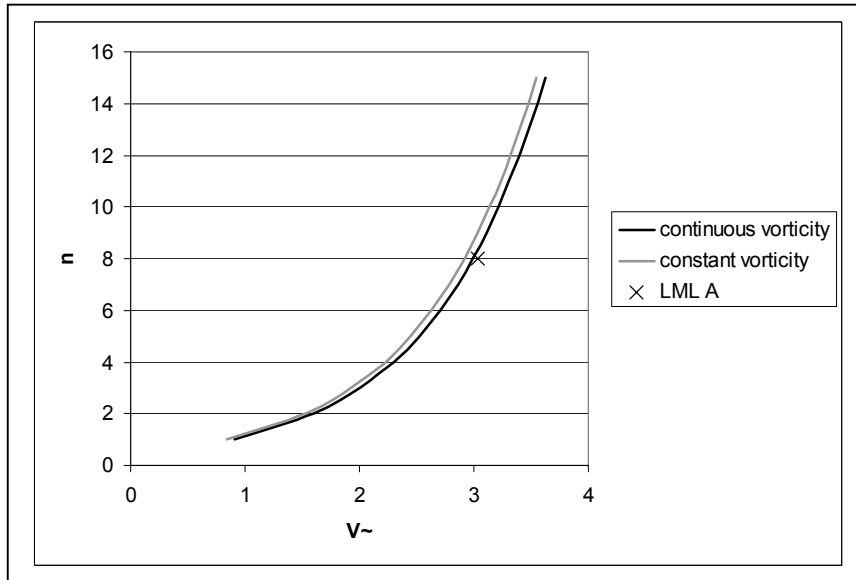


Figure 16: Theoretical and experimental results

5-Non-linear phase

Following the linear phase of development, more or less rapidly depending on the Reynolds number, a non linear phase occur in the evolution of the vortex ring. The first non linear visible effects occur in the median plane of the vortex. Vortical structures, in the same number as the number of waves of the initial unstable mode spring up (figure 17 b) at the edges of the vortex, and develop outward (figure 17 c).

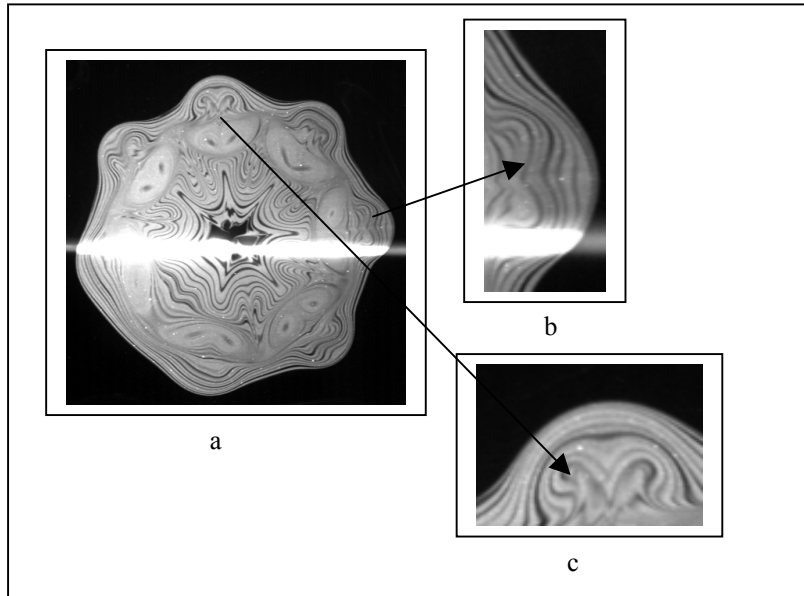


Figure 17: $Re = 3800$; $L_p/D_p = 1.25$ $t = 5.83$ s $z_c = 0$
Vortical structures: (b) arising - (c) fully developed

They then extend around the median plane; in the upstream (figure 18) and in the downstream parts of the vortex (figure 19).

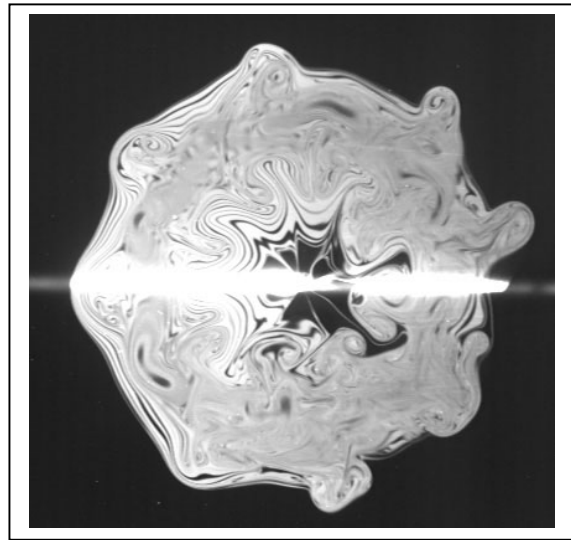
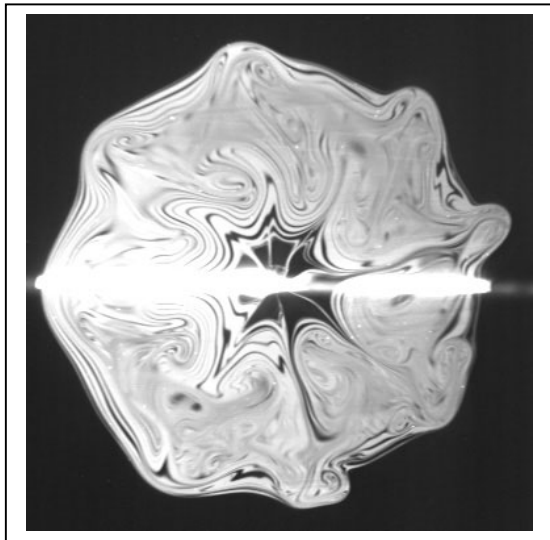
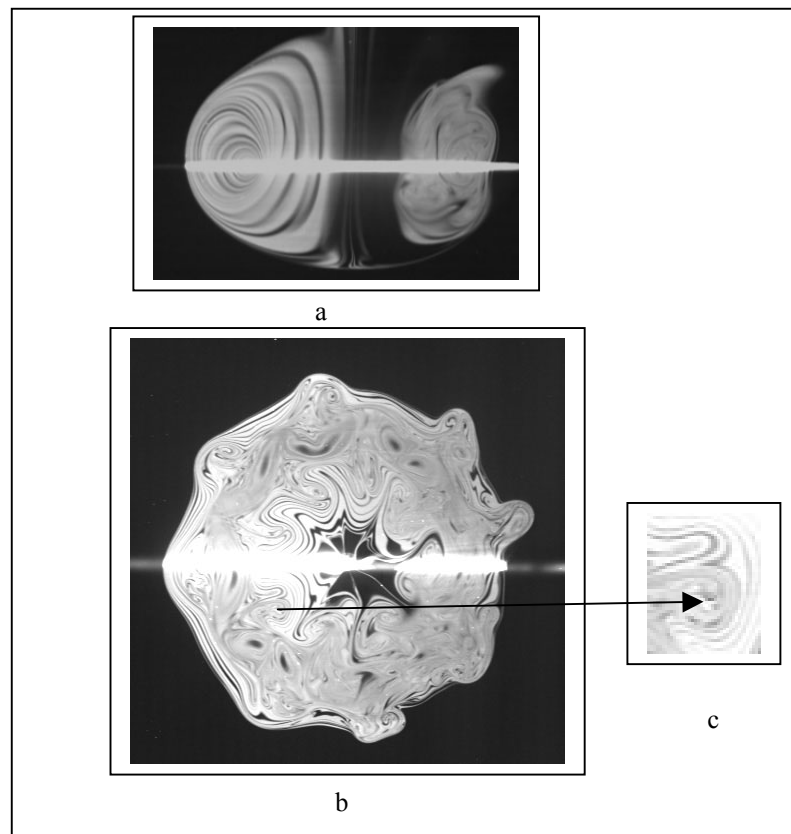


Figure 18: $Re = 4900$ $L_p/D_p = 1.95$ $t = 4.23$ s $z_c = -0.2$ **Figure 19: $Re = 4900$ $L_p/D_p = 1.95$ $t = 4.37$ s $z_c = 0.2$**

This phase is characterised by a progressive loss of symmetry and by the development of secondary vortical structures in the inner part of the vortex too (figure 20b, 20c).



a: V plane, b: H plane, c: detail

In the V plane (figure 20a), even if the instability is now obvious on one side of the ring, the vortex seems steadier than it is really, according to the observations in the H plane. The non-linear phase of the instability leads quickly to the destruction of the ring.

6-Conclusion

The analysis of tomographic images of experimentally produced vortex rings has evidenced two phases during the development of the instability. A linear phase during which the patterns experimentally observed (Type I to Type VI) are the consequence of the existence of a three dimensional azimuthal wave developing around the initially stable vortex ring. A geometrical model allows to clearly link the observed patterns to the perturbation. The PIV results confirm the existence of an azimuthal wave around the ring. The number of waves observed in the PIV experiments is in good agreement with the theoretical model of Widnall et al (1977).

The non-linear phase of the instability is characterised by the formation of secondary vortical structures. This phases come just before the destruction of the ring.

A more elaborate analysis of the PIV results and of some stereo-PIV experiments which are under way should allow a more quantitative study of the instability phenomena. In the linear phase, it should allow to calculate the growth rate of the perturbation in order to compare it with theory. It should also allow to better understand the non-linear phase of the instability.

References

Crow 1970
Stability theory for a pair of trailing vortices
AIAA 8, 2172

N.Didden 1979
On the formation of Vortex rings: Rolling-up and Production of Circulation
Journal of Applied Mathematics and Physics 30, 101-116

- C.C Chu, R.E Falco 1988
Vortex ring/viscous wall layer interaction model of the turbulence production process near a wall
Experiment in Fluids 6, 305-315
- A.Glezer 1988
The formation of vortex rings
Physics of Fluids 31,12 3532-3542
- T.Maxworthy 1972
The structure and stability of vortex rings,
JFM 51, 15-32
- T.Maxworthy 1977
Some experimental studies of vortex rings,
JFM 81 465-495
- H.Meng, F.Hussein 1995
Instantaneous flow field in an unstable vortex ring measured by holographic particle image velocimetry
Physics of Fluids 7 9-11
- P. Orlandi, R. Verzicco 1993
Vortex rings impinging on walls: axisymmetric and three-dimensional simulation
JFM 256 615-646
- K. Shariff, R. Verzicco, P. Orlandi 1994
A numerical study of three-dimensional vortex ring instabilities: viscous correction and early non-linear stage.
JFM vol 279, pp351-375
- P.G.Saffman 1978
The number of waves on unstable vortex rings,
JFM 84 721-733
- P.G Saffman 1981
Dynamics of vorticity
JFM vol 106, pp49-58.
- J.P Sullivan, S.E Widnall, S.Ezekiel 1973
Study of vortex rings using a Laser Doppler Velocimeter
AIAA vol 11, n10 pp 1384-1389
- C.Y Tsai; S.E Widnall 1976
The stability of short waves on a straight vortex filament in a weak externally imposed strain field
JFM vol 73, pp 721-733
- S.E Widnall, J.P Sullivan, S. Ezekiel 1973
On the stability of vortex rings.
Proc.Roy.Soc.A. 332 pp335-353
- S.E Widnall, D.B.Bliss, C.Y Tai, 1974
The instability of short waves on a vortex ring,
JFM 66 (1974) 35-47
- S.E Widnall, C.Y Tsai 1977
The instability of the thin vortex ring of constant vorticity
PH.Trans.of.Roy.Soc.London, a (1977) 287,pp273-305